Enantioselective metabolism of chiral polychlorinated biphenyl 2,2′,3,4,4′,5′,6-Heptachlorobiphenyl (CB183) by human and rat CYP2B subfamilies

Ito, Terushi ; Miwa, Chiharu ; Haga, Yuki ; Kubo, Makoto ; Itoh, Toshimasa ; Yamamoto, Keiko ; Mise, Shintaro ; Goto, Erika ; Tsuzuki,…

(Citation)
Chemosphere,308(2):136349

(Issue Date)
2022-09-06

(Resource Type)
journal article

(Version)
Accepted Manuscript

ABSTRACT

Chiral polychlorinated biphenyls (PCBs) have atropisomers that have different axial chiralities and exist as racemic mixtures. However, biochemical processes often result in the unequal accumulation of these atropisomers in organisms. This phenomenon leads to enantiospecific toxicity enhancement or reduction because either of the atropisomers mainly affects toxicity expression. Enantioselective accumulation is caused by cytochrome P450 (CYP, P450) monooxygenases, especially the CYP2B subfamilies. Therefore, this study investigates the metabolism of a chiral PCB *in vitro*. Both atropisomers isolated from racemic 2,2′,3,4,4′,5′,6-heptachlorobiphenyl (CB183) were metabolized by human CYP2B6, but not rat CYP2B1. This may be due to the difference in the size of the substrate-binding cavities of CYP2B6 and CYP2B1. The stable accommodation of (–)-CB183 in the cavity without any steric hindrance explained the preferential metabolism of (–)-CB183 compared to (+)-CB183. Two hydroxylated metabolites, 3′-OH-CB183 and 5-OH-CB183, were identified. The docking study showed that the 3′-position of the trichlorophenyl ring closely approaches the heme of CYP2B6. To our knowledge, this is the first study to elucidate the structural basis of chiral PCB metabolism by P450 isozymes. These results will help promote the precise toxicity evaluation of chiral PCBs and provide an explanation of the structural basis of chiral PCB metabolism.

Keywords: atropisomer, chiral polychlorinated biphenyl, cytochrome P450 monooxygenase, enantioselective metabolism, CB183

1. Introduction

Polychlorinated biphenyls (PCBs) have been widely used in industrial products like insulating oils for electrical machinery, transmitters, and condensers owing to their incombustibility and insulation properties. PCBs are known as legacy persistent organic pollutants (POPs) and continuous efforts are being made to eliminate their production and usage. Yet, environmental contamination (Zhu et al., 2022) due to PCBs and instances of their bioaccumulation in humans and wildlife are frequently reported (Quinete et al., 2014). Multiple adverse effects of PCBs on human health are known, such as carcinogenicity, reproductive impairment, and developmental neurotoxicity. Of the 209 PCB congeners, 19 PCB congeners that have either three or four *ortho* chlorine substituents display axial chirality and are called chiral PCBs. Generally, atropisomers of chiral PCBs that are non-superimposable mirror images of each other exist as racemic mixtures in the environment and have identical physical and chemical properties. However, they show different metabolism, accumulation, and toxicity *in vivo* because of their different three-dimensional structures. 2,2′,3,4,4′,5′,6-Heptachlorobiphenyl (CB183) was reported to accumulate enantioselectively in human breast milk and adipose tissue, suggesting that the concentration of one atropisomer is lower *in vivo* (Bordajandi et al., 2008; Konishi et al., 2016; Toda et al., 2012). Mammalian cytochrome P450 (CYP or P450) monooxygenases are known to metabolize various PCB congeners. Rat CYP1A1 metabolizes the most toxic PCB congener 3,3′,4,4′,5-pentachlorobiphenyl (CB126) to hydroxylated metabolites (Yamazaki et al., 2011). Docking models of CB126 with CYP1A1 revealed that the 4-OH-3,3′,4′,5-tetrachlorobiphenyl metabolite is formed because CB126 occupies the active site of CYP1A1 in such a manner that its 4-position is closest to the heme iron. In contrast, 2,3′,4,4′,5-pentachlorobiphenyl (CB118) is metabolized by human and rat CYP2B subfamilies (Mise et al., 2016). Docking studies

showed that CB118 is positioned closer to the heme iron of human CYP2B6 compared to that of rat CYP2B1. Therefore, human CYP2B6 produces higher amounts of hydroxylated metabolites. These studies suggest that the stable accommodation of PCBs in the substrate-binding cavities of P450s and their vicinity to the heme iron are responsible for the high PCB metabolism. The CYP2B subfamily has also been employed for the enantioselective metabolism of chiral PCBs. While both rat CYP2B1 and human CYP2B6 biotransformed 2,2′,3,6-tetrachlorobiphenyl (CB45) to hydroxylated metabolites, they showed a different atropisomer preference that reflected in the opposite enantiomer fractions obtained for the two isozymes (Warner et al., 2009). Furthermore, CYP2B-induced rat liver microsomes preferentially metabolized (+)-CB136 to (+)-5-OH-CB136 (Wu et al., 2011).

Enantioselective binding activities of 2,2′,3,5′,6-pentachlorobiphenyl (CB95) atropisomers toward a ryanodine receptor (RyR) were also observed (Feng et al., 2017). (–)-CB95 showed a higher binding activity toward RyR than its racemate, leading to enantiomer-specific toxicity. The same phenomenon was observed in the case of (–)-2,2′,3,3′,6,6′-hexachlorobiphenyl (CB136), which acts as a sensitizer toward RyR and causes neurodevelopmental toxicity (Yang et al., 2014). Therefore, it is important to further explore the enantioselective metabolism of chiral PCBs by P450 isozymes, especially by the CYP2B subfamily, since PCB toxicity is dependent on metabolism. Chiral CB183 is one of the most potent congeners to activate the RyR-Ca^{2+} channel complex type 1 (Holland et al., 2017; Pessah et al., 2006). This receptor is regulating a cellular signaling through calcium release. Therefore, clarification of its metabolic fate is of great interest. It was reported that the serum, feces, and liver microsomes from CYP2B-induced rats showed the production of 3′-OH-CB183 and 5-OH-CB183 (Ohta et al., 2007,

2006). However, the enantioselective metabolism of CB183 and its structural basis have not been explored.

In this study, we show the enantioselective metabolism of CB183 atropisomers by human and rat CYP2B subfamilies *in vitro*. Separated atropisomers (Figure 1) were used as substrates of P450 isozymes in metabolism experiments. This study reveals several important aspects of the enantioselective metabolism of CB183, which will allow an adequate evaluation of its toxicity. Furthermore, docking models of CB183 atropisomers and the human CYP2B6 reveal the structural basis underlying its enantioselective metabolism.

2. Materials and methods

2.1. Chemicals

The two atropisomers were separated from racemic CB183 (AccuStandard, New Haven, CT) by chiral HPLC on a CHIRALCEL® OJ-H column (Daicel Co., Osaka, Japan) under the conditions reported previously (Toda et al., 2012). Each of the atropisomers were dissolved in dimethyl sulfoxide to achieve a final concentration of 0.25 mM. ^{13}C-labeled OH-PCBs (MHPCB-MXA: [$^{13}C_{12}$]-4-Hydroxy-3′,4′-dichlorobiphenyl, [$^{13}C_{12}$]-4-hydroxy-2′,4′,5′-trichlorobiphenyl, [$^{13}C_{12}$]-4-hydroxy-2′,3′,4′,5′-tetrachlorobiphenyl, [$^{13}C_{12}$]-4-hydroxy-2′,3,4′,5,5′-pentachlorobiphenyl, [$^{13}C_{12}$]-4-hydroxy-2′,3,3′,4′,5,5′-hexachlorobiphenyl, [$^{13}C_{12}$]-4-hydroxy-2,2′,3,3′,4′,5,5′-heptachlorobiphenyl, and [$^{13}C_{12}$]-4-hydroxy-2,2′,3,4′,5,5′,6-heptachlorobiphenyl), used as internal standards, and [$^{13}C_{12}$]-2,3′,4′,5-tetrachlorobiphenyl, used as the syringe spike, were purchased from Wellington Laboratories (Guelph, Canada). The 3′-OH-CB183 and 5-OH-CB183 standards were kindly provided by Dr. T. Okumura (Environmental

97 Pollution Control Center, Osaka Prefecture, Osaka, Japan). Microsomes containing
98 NADPH-cytochrome P450 oxidoreductase (CPR) and cytochrome b_5, along with human
99 CYP2B6 or rat CYP2B1 that are heterologously produced in recombinant insect cells
100 were purchased from BD Biosciences (San Jose, CA, USA).
101 *2.2. Measurement of hydroxylation activity of CYP2B subfamilies toward CB183*
102 The reaction solution contained 2.5 μM (+)- or (–)-CB183, 80 nM human CYP2B6 or
103 rat CYP2B1, 3.3 mM $MgCl_2$, 100 mM potassium phosphate buffer (pH 7.4), NADPH
104 regenerating system (5 mM NADPH, 5 mM glucose-6-phosphate, 1 unit glucose-6-
105 phosphate dehydrogenase) in a total volume of 0.5 mL. The reaction was initiated by
106 adding a microsomal fraction and was incubated for 120 min at 37 °C with continuous
107 shaking. Control experiments were performed using the same procedure without the
108 addition of NADPH. The reaction was terminated moving the tubes containing the
109 reaction mixture on ice, and 20 μL of 50 ng/mL ^{13}C-OH-PCB was added as an internal
110 standard. The metabolites were extracted twice with 2 mL of hexane and derivatized by
111 methylation as described previously (Sakiyama et al., 2007). Quantification and
112 identification of the metabolites (Table S1–S3 of Supplementary Information) were
113 performed by high-resolution gas chromatography and high-resolution mass
114 spectrometry (HRGC/HRMS: GC, 6890N [Agilent Technologies, Tokyo, Japan]; MS,
115 JMS-800D [JEOL Ltd., Tokyo, Japan]) equipped with an HT8-PCB column (Kanto
116 Chemical Co. Inc., Tokyo, Japan) using SIM modes under the conditions described
117 previously (Goto et al., 2018). The identification of retention times between metabolites
118 and the authentic standards, and isotope ratios ($[M+2]^+$:$[M+4]^+$) of MeO-
119 heptachlorobiphenyls were employed to identify OH-PCBs. Relative calibration curves
120 that are prepared by the division of the peak areas of different concentrations of 5-MeO-

CB183 by that of [$^{13}C_{12}$]-4-MeO-2,2′,3,4′,5,5′,6-heptachlorobiphenyl were used to quantify M1 and M2. The recovery rates for metabolites were calculated by using an internal standard and syringe spikes as 57–125% for hydroxylated heptachlorobiphenyls.

2.3. Molecular docking of CB183 in the substrate-binding site of human CYP2B6

Both atropisomers of CB183 were docked in the substrate-binding site of human CYP2B6 using Surflex Dock in SYBYL 8.0 (Tripos, St Louis, MO) (Gay et al., 2010; Ruppert et al., 1997). To determine a reasonable conformation of CB183, 13 crystal structures of human CYP2B6 stored in the Protein Data Bank (PDB IDs: 3IBD, 3QOA, 3QU8, 3UA5, 4I91, 4RQL, 4RRT, 4ZV8, 5EM4, 5UAP, 5UDA, 5UEC, and 5UFG) were superimposed.

3. Results and discussion

3.1. Detection and identification of CB183 metabolites

In microsomes containing human CYP2B6, two different NADPH-dependent hydroxylated heptachloro metabolites (M1 and M2) were detected for both the atropisomers by HRGC/HRMS (Figure 2B–E). In contrast, no metabolites were detected in rat CYP2B1 for both isomers (Figure 2F–I). A possible reason for this could be the different volumes of the substrate-binding cavities of rat CYP2B1 (472 Å) and human CYP2B6 (559 Å) (Mise et al., 2016). This is an important factor when considering the stable accommodation of substrates in the binding site, which is responsible for the varying metabolizing activities of the different P450 isozymes. This suggests that the binding cavity of rat CYP2B1 is too small to accommodate the heptachlorinated CB183. However, rat CYP2B1 has been reported to metabolize hexachlorinated PCB congeners, such as 2,2′,3,3′,4,6′-hexachlorobiphenyl (CB132) and CB136 to hydroxylated products,

which suggests that the binding site of rat CYP2B1 can only accommodate up to hexachlorinated PCBs (Warner et al., 2009). Yet, in a contradictory report, 3′-OH-CB183 and 5-OH-CB183 were detected in the serum of rats intraperitoneally dosed with phenobarbital as a CYP2B inducer, followed by CB183 (Ohta et al., 2007). This contradiction can be attributed to the different experimental conditions as one study was conducted *in vitro* and the other *in vivo.* CYP2B1 is a frequently used isoform among rat CYP2B subfamilies for *in vitro* experiments. However, there are other CYP2B subfamilies in rats, such as CYP2B2, CYP2B3, CYP2B12, CYP2B15, and CYP2B21. Therefore, it is possible that CB183 is metabolized by other rat CYP2B subfamilies.

As the retention time of methylated M1 was consistent with that of the authentic standard S1 (3′-MeO-CB183), M1 was identified as 3′-OH-CB183 (Table S2). Similarly, M2 was identified as 5-OH-CB183. Their peaks also matched the isotope ratios ($[M+2]^+$:$[M+4]^+$) of MeO-heptachlorobiphenyl, indicating that the peaks represent hydroxylated heptachloro compounds (Figure S1, Table S3). According to the fragmentation patterns of the CB183 metabolites, M1 and M2 had larger peaks in $[M+2\text{-}COCH_3]^+$ than in $[M+2\text{-}CH_3Cl]^+$ (Figure S2). The peak of $[M+2\text{-}COCH_3]^+$ indicated that the substituted hydroxyl group was located at the *meta*- or *para*-position (Kunisue and Tanabe, 2009). This result was consistent with the identification of M1 as 3′-OH-CB183 and M2 as 5-OH-CB183. Further, CYP2B subfamilies preferentially hydroxylate at *meta*-position of PCBs whereas CYP1A1 preferentially hydroxylates at *para*-position (Mise et al., 2016). 3′-OH-CB183 and 5-OH-CB183 were also detected in the serum of rats injected with CB183 and the concentration of these metabolites increased due to the presence of phenobarbital (Ohta et al., 2007). These reports support our observation that CB183 can be metabolized to 3′-OH-CB183 and 5-OH-CB183 by the CYP2B subfamily.

169 *3.2. Production rates of hydroxylated CB183 by human CYP2B6*

170 Higher concentrations of metabolites were obtained in case of (–)-CB183 compared to
171 (+)-CB183, with the concentration of 3′-OH-CB183 being 5.5 times higher and that of 5-
172 OH-CB183 being 4.3 times higher (Figure 3). The production rates of 3′-OH-CB183 from
173 (+)-CB183 and (–)-CB183 were 2.7 and 3.5 times higher than those of 5-OH-CB183,
174 respectively. The proposed metabolic pathways of CB183 are shown in Figure 4. It has
175 been reported that (+)-CB183 is more abundant than (–)-CB183 in human breast milk,
176 while a racemic CB183 is present in fish, which is a major source of PCB intake (Konishi
177 et al., 2016). These results suggest that CYP2B6 is related to the metabolism of (–)-
178 CB183 in the human body. In contrast, it was reported that human CYP2B6 did not show
179 enantioselective metabolism of racemic CB183 (Nagayoshi et al., 2018; Warner et al.,
180 2009). This suggests that atropisomers influence each other's metabolism. This
181 hypothesis is supported by the study in which (–)-CB132 inhibited the biotransformation
182 of (+)-CB132 in the racemic mixture owing to the difference in the binding affinity of
183 each atropisomer toward rat CYP2B1 (Lu and Wong, 2011).

184 *3.3. Docking models of CB183 with human CYP2B6*

185 To understand the molecular basis of enantioselective metabolism and different
186 production rates of the two metabolites, both the atropisomers of CB183 were docked in
187 the substrate-binding cavity of human CYP2B6 (PDB ID: 3IBD) (Figure S3A). The 13
188 crystal structures of human CYP2B6 obtained from PDB were superimposed to identify
189 the substrate-binding cavity of human CYP2B6 (Figure S3B). Binding modes of eight
190 conformations showed that either the 3′- or 5-position of CB183 approaches the heme
191 iron in the substrate-binding cavity (Figure S3A). From these results, a plausible
192 conformation of CB183 (displayed in red) in the cavity was selected (Figure S3A). Our

193 docking models indicate that the (–)-CB183 conformation experiences no steric hindrance
194 in the substrate-binding cavity (Figure 5A). In contrast, steric hindrance between Cl at 3-
195 position of (+)-CB183 and the cavity was observed (Figure 5B). Bulky side chains of
196 amino acids I101, I209, and V474 were positioned 2.8, 2.9, and 3.3 Å away from the Cl
197 residue at 3-postion, respectively (Figure 5C). This adversely affects the conformational
198 stability of (+)-CB183, resulting in its lower metabolizing activity. In the future studies,
199 a binding energy calculated in the docking simulation is compared between human
200 CYP2B6 or rat CYP2B1 and atropisomers of CB183 to support these models.
201 The selective production of two metabolites could be associated with two factors.
202 Firstly, CB183 has seven chlorines and is composed of a trichlorophenyl and a
203 tetrachlorophenyl ring (Figure 1). The electrostatic potential map of CB183 is shown in
204 Figure S4. The tetrachorophenyl ring is electron-deficient due to the presence of four
205 electron-withdrawing chlorine groups, whereas the trichlorophenyl ring has three
206 chlorines, making it relatively electron-rich, which facilitates the reaction at 3′-position.
207 The dipole moment of the tetrachloro-substituted phenyl ring was larger than that of the
208 trichloro-substituted ring. Therefore, it is possible that dipole-induced dipole interactions
209 occur in the lipophilic area (Figure 6A). Conversely, when a trichlorophenyl ring occupies
210 the right side of the cavity, the stability is decreased, causing low hydroxylation activity
211 at the 5-position (Figure 6B). Thus, the preferential metabolism of (–)-CB183
212 atropisomer to the 3′-OH-CB183 metabolite by human CYP2B6 can be explained by
213 these docking models.
214

215 **4. Conclusions**

All chiral PCBs are considered to have no dioxin-like toxicity because the expression of dioxin-like toxicity requires a co-planar structure that does not contain chlorine or has only one chlorine at *the ortho*-position. However, chiral PCBs alter calcium regulation associated with neuronal signaling through RyR (Wong and Pessah, 1996). (–)-CB95 and (–)-CB136 are known to cause enantioselective neurodevelopmental toxicity via RyR (Feng et al., 2017; Yang et al., 2014). Since CB183 also has RyR-binding activity, enantioselective binding activities of CB183 atropisomers have been observed (Pessah et al., 2006). Furthermore, it has been reported that chiral PCBs with a hydroxyl group, especially at *the meta*-position, decrease the binding activity toward RyR. These results suggest that hydroxylation of chiral PCBs by P450 species plays an important role in decreasing toxicity. Atropisomer-specific binding activity of CB183 toward RyR should be examined to understand how human CYP2B6 alters toxicity patterns.

In this study, we have shown that the atropisomers of chiral CB183 are metabolized to 3′- and 5-hydroxylated heptachloro metabolites by human CYP2B6. Furthermore, (–)-CB183 was metabolized to a greater extent than (+)-CB183. These observations were explained with the help of docking models of CB183 atropisomers with human CYP2B6. To our knowledge, this is the first study to explore the structural basis of chiral PCB metabolism by P450 species. Our results will accelerate research on the clarification of the structural basis of chiral PCB metabolism and precise toxicity evaluation of chiral PCBs. In addition to the biotransformation of chiral PCBs, factors like differences in the binding activity of transporter proteins toward chiral PCBs and cell membrane permeability should be taken into consideration for enantiomeric enrichment of chiral PCBs (Nagayoshi et al., 2018).

Acknowledgements

We thank Dr. Tameo Okumura of Environmental Pollution Control Center Osaka Prefecture, Osaka, Japan for kindly providing us with the standards 3′-OH-CB183 and 5-OH-CB183.

Funding Sources

This work was supported by a Grant-in-Aid for Challenging Exploratory Research (grant number: 25550064) from the Japan Society for the Promotion of Science.

References

Bordajandi, L.R., Abad, E., González, M.J., 2008. Occurrence of PCBs, PCDD/Fs, PBDEs and DDTs in Spanish breast milk: Enantiomeric fraction of chiral PCBs. Chemosphere 70, 567–575. https://doi.org/10.1016/j.chemosphere.2007.07.019

Feng, W., Zheng, J., Robin, G., Dong, Y., Ichikawa, M., Inoue, Y., Mori, T., Nakano, T., Pessah, I.N., 2017. Enantioselectivity of 2,2′,3,5′,6-Pentachlorobiphenyl (PCB 95) Atropisomers toward Ryanodine Receptors (RyRs) and Their Influences on Hippocampal Neuronal Networks. Environ. Sci. Technol. 51, 14406–14416. https://doi.org/10.1021/acs.est.7b04446

Gay, S.C., Shah, M.B., Talakad, J.C., Maekawa, K., Roberts, A.G., Wilderman, P.R., Sun, L., Yang, J.Y., Huelga, S.C., Hong, W.X., Zhang, Q., Stout, C.D., Halpert, J.R., 2010. Crystal structure of a cytochrome P450 2B6 genetic variant in complex with the inhibitor 4-(4-chlorophenyl)imidazole at 2.0-Å resolution. Mol. Pharmacol. 77, 529–538. https://doi.org/10.1124/mol.109.062570

263 Goto, E., Haga, Y., Kubo, M., Itoh, T., Kasai, C., Shoji, O., Yamamoto, K., Matsumura,
264 C., Nakano, T., Inui, H., 2018. Metabolic enhancement of 2,3″,4,4″,5-
265 pentachlorobiphenyl (CB118) using cytochrome P450 monooxygenase isolated
266 from soil bacterium under the presence of perfluorocarboxylic acids (PFCAs) and
267 the structural basis of its metabolism. Chemosphere 210, 376–383.
268 https://doi.org/10.1016/j.chemosphere.2018.07.026
269 Holland, E.B., Feng, W., Zheng, J., Dong, Y., Li, X., Lehmler, H.J., Pessah, I.N., 2017.
270 An extended structure-Activity relationship of nondioxin-like PCBs evaluates and
271 supports modeling predictions and identifies picomolar potency of PCB 202
272 towards ryanodine receptors. Toxicol. Sci. 155, 170–181.
273 https://doi.org/10.1093/toxsci/kfw189
274 Konishi, Y., Kakimoto, K., Nagayoshi, H., Nakano, T., 2016. Trends in the
275 enantiomeric composition of polychlorinated biphenyl atropisomers in human
276 breast milk. Environ. Sci. Pollut. Res. 23, 2027–2032.
277 https://doi.org/10.1007/s11356-015-4620-6
278 Kunisue, T., Tanabe, S., 2009. Hydroxylated polychlorinated biphenyls (OH-PCBs) in
279 the blood of mammals and birds from Japan: Lower chlorinated OH-PCBs and
280 profiles. Chemosphere 74, 950–961.
281 https://doi.org/10.1016/j.chemosphere.2008.10.038
282 Lu, Z., Wong, C.S., 2011. Factors affecting phase i stereoselective biotransformation of
283 chiral polychlorinated biphenyls by rat cytochrome P-450 2B1 isozyme. Environ.
284 Sci. Technol. 45, 8298–8305. https://doi.org/10.1021/es200673q
285 Mise, S., Haga, Y., Itoh, T., Kato, A., Fukuda, I., Goto, E., Yamamoto, K., Yabu, M.,
286 Matsumura, C., Nakano, T., Sakaki, T., Inui, H., 2016. Structural determinants of

the position of 2,3',4,4',5-pentachlorobiphenyl (CB118) hydroxylation by mammalian cytochrome P450 monooxygenases. Toxicol. Sci. 152, 340–348. https://doi.org/10.1093/toxsci/kfw086

Nagayoshi, H., Kakimoto, K., Konishi, Y., Kajimura, K., Nakano, T., 2018. Determination of the human cytochrome P450 monooxygenase catalyzing the enantioselective oxidation of 2,2′,3,5′,6-pentachlorobiphenyl (PCB 95) and 2,2′,3,4,4′,5′,6-heptachlorobiphenyl (PCB 183). Environ. Sci. Pollut. Res. 25, 16420–16426. https://doi.org/10.1007/s11356-017-0434-z

Ohta, C., Haraguchi, K., Kato, Y., Matsuoka, M., Endo, T., Koga, N., 2007. THE DISTRIBUTION OF METABOLITES OF 2,2',3,4,4',5',6-HEPTACHLOROBIPHENYL (CB183) IN RATS AND GUINEA PIGS. Organohalogen Compd. 69, 1761–1764. https://doi.org/10.13040/IJPSR.0975-8232.7(6).2573-85

Ohta, C., Haraguchi, K., Kato, Y., Ozaki, M., Koga, N., 2006. Biochemical and molecular mechanisms (CB183) WITH LIVER MICROSOMES FROM RATS , GUINEA PIGS AND HAMSTERS Organohalogen Compounds Vol 68 (2006) A) Rat B) Guinea pig C) Hamster Organohalogen Compounds Vol 68 (2006). Organohalogen Compd. 68, 1733–1736.

Pessah, I.N., Hansen, L.G., Albertson, T.E., Garner, C.E., Ta, T.A., Do, Z., Kim, K.H., Wong, P.W., 2006. Structure-activity relationship for noncoplanar polychlorinated biphenyl congeners toward the ryanodine receptor-Ca 2+ channel complex type 1 (RyR1). Chem. Res. Toxicol. 19, 92–101. https://doi.org/10.1021/tx050196m

Quinete, N., Schettgen, T., Bertram, J., Kraus, T., 2014. Occurrence and distribution of PCB metabolites in blood and their potential health effects in humans: a review.

311 Environ. Sci. Pollut. Res. 21, 11951–11972. https://doi.org/10.1007/s11356-014-
312 3136-9
313 Ruppert, J., Welch, W., Jain, A.N., 1997. Automatic identification and representation of
314 protein binding sites for molecular docking. Protein Sci. 6, 524–533.
315 https://doi.org/10.1002/pro.5560060302
316 Sakiyama, T., Yamamoto, A., Kakutani, N., Fukuyama, J., and Okumura, T., 2007.
317 Hydroxylated polychlorinated biphenyls (OH-PCBs) in the aquatic environment:
318 Levels and congener profiles in sediments from Osaka. Japan. Organohal. Comp.
319 69, 1380–1383.
320 Toda, M., Matsumura, C., Tsurukawa, M., Okuno, T., Nakano, T., Inoue, Y., Mori, T.,
321 2012. Absolute configuration of atropisomeric polychlorinated biphenyl 183
322 enantiomerically enriched in human samples. J. Phys. Chem. A 116, 9340–9346.
323 https://doi.org/10.1021/jp306363n
324 Warner, N.A., Martin, J.W., Wong, C.S., 2009. Chiral polychlorinated biphenyls are
325 biotransformed enantioselectively by mammalian cytochrome P-450 isozymes to
326 form hydroxylated metabolites. Environ. Sci. Technol. 43, 114–121.
327 https://doi.org/10.1021/es802237u
328 Wong, P., Pessah, I.N., 1996. Ortho-substituted polychlorinated biphenyls alter calcium
329 regulation by a ryanodine receptor-mediated mechanism: structural specificity
330 toward skeletal- and cardiac-type microsomal calcium release channels. Mol.
331 Pharmacol. 49, 740–751.
332 Wu, X., Pramanik, A., Duffel, M.W., Hrycay, E.G., Bandiera, S.M., Lehmler, H.,
333 Kania-korwel, I., 2011. Oxidized to Hydroxylated Metabolites by Rat Liver
334 Microsomes 2249–2257.

335 Yamazaki, K., Suzuki, M., Itoh, T., Yamamoto, K., Kanemitsu, M., Matsumura, C.,
336 Nakano, T., Sakaki, T., Fukami, Y., Imaishi, H., Inui, H., 2011. Structural basis of
337 species differences between human and experimental animal CYP1A1s in
338 metabolism of 3,3′,4,4′,5-pentachlorobiphenyl. J. Biochem. 149.
339 https://doi.org/10.1093/jb/mvr009
340 Yang, D., Kania-Korwel, I., Ghogha, A., Chen, H., Stamou, M., Bose, D.D., Pessah,
341 I.N., Lehmler, H.J., Lein, P.J., 2014. PCB 136 atropselectively alters morphometric
342 and functional parameters of neuronal connectivity in cultured rat hippocampal
343 neurons via ryanodine receptor-dependent mechanisms. Toxicol. Sci. 138, 379–
344 392. https://doi.org/10.1093/toxsci/kft334
345 Zhu, M., Yuan, Y., Yin, H., Guo, Z., Wei, X., Qi, X., Liu, H., Dang, Z., 2022.
346 Environmental contamination and human exposure of polychlorinated biphenyls
347 (PCBs) in China: A review. Sci. Total Environ. 805, 150270.
348 https://doi.org/10.1016/j.scitotenv.2021.150270
349
350

Figures

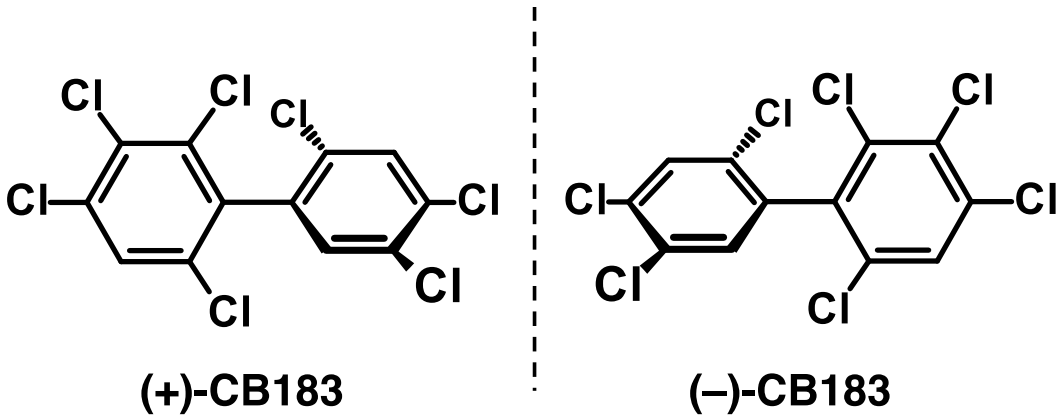

Figure 1 Chemical structures of atropisomers of 2,2′,3,4,4′,5′,6-heptachlorobiphenyl (CB183).

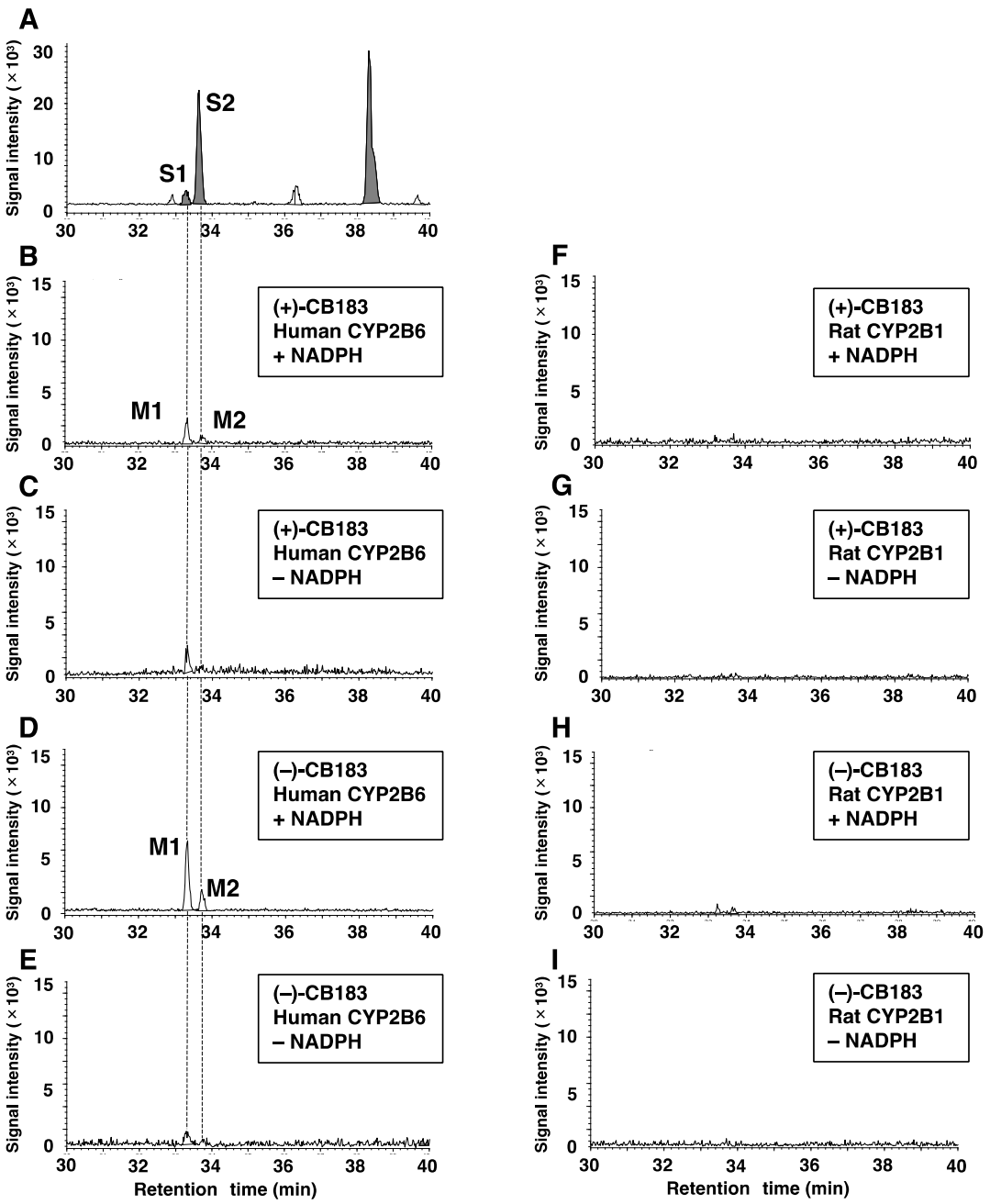

Figure 2 Chromatograms of hydroxylated heptachloro metabolites of CB183 by human CYP2B6 and rat CYP2B1 analyzed by high-resolution gas chromatography/high-resolution mass spectrometry.

(A): S1 and S2 are the authentic standards 3′-MeO-CB183 and 5-MeO-CB183, respectively. (B) and (C): Metabolism of (+)-CB183 by human CYP2B6, with and without NADPH, respectively. (D) and (E): Metabolism of (–)-CB183 by human CYP2B6, with and without NADPH, respectively. (F) and (G): Metabolism of (+)-CB183

by rat CYP2B1, with and without NADPH, respectively. (H) and (I): Metabolism of (–)-CB183 by rat CYP2B1, with and without NADPH, respectively. Metabolites are represented as M1 and M2, respectively.

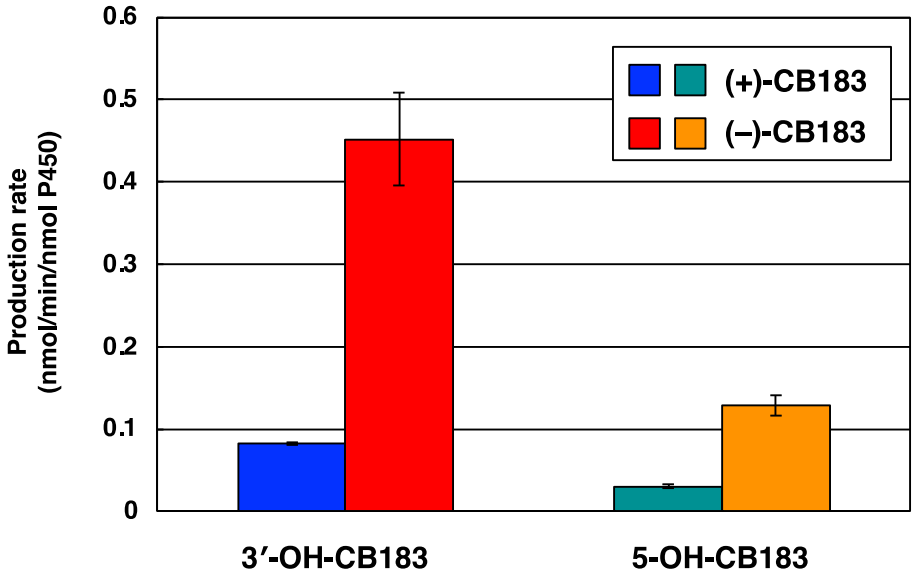

Figure 3 Production rates of CB183 metabolites by human CYP2B6. Data were presented as mean ± standard deviation (n = 4).

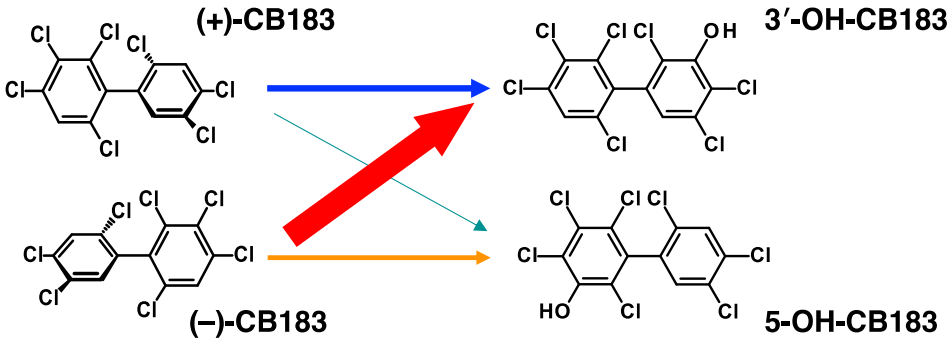

Figure 4 Proposed metabolic pathways of CB183 atropisomers by human CYP2B6. Enantioselective metabolism is shown by arrow thickness, which indicates the level of hydroxylation activity.

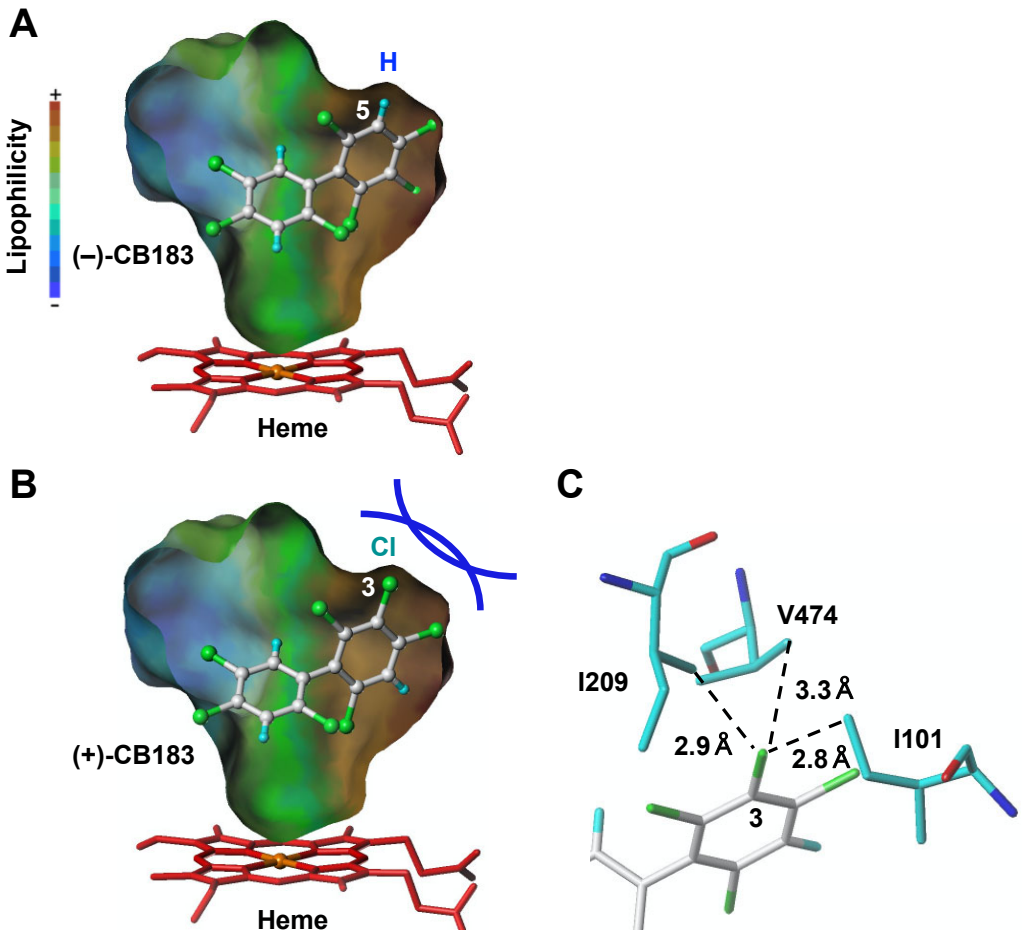

Figure 5 Preferential metabolism of (–)-CB183 by human CYP2B6.
Docking models of (–)-CB183 (A) and (+)-CB183 (B) in the binding cavity of human CYP2B6. Blue and green spheres in CB183 indicate the hydrogen and chlorine atoms, respectively. Steric hindrance between the Cl atom at 3-position of (+)-CB183 and bulky side chains of amino acids I101, I209, and V474 that are present in the human CYP2B6 cavity is observed (C).

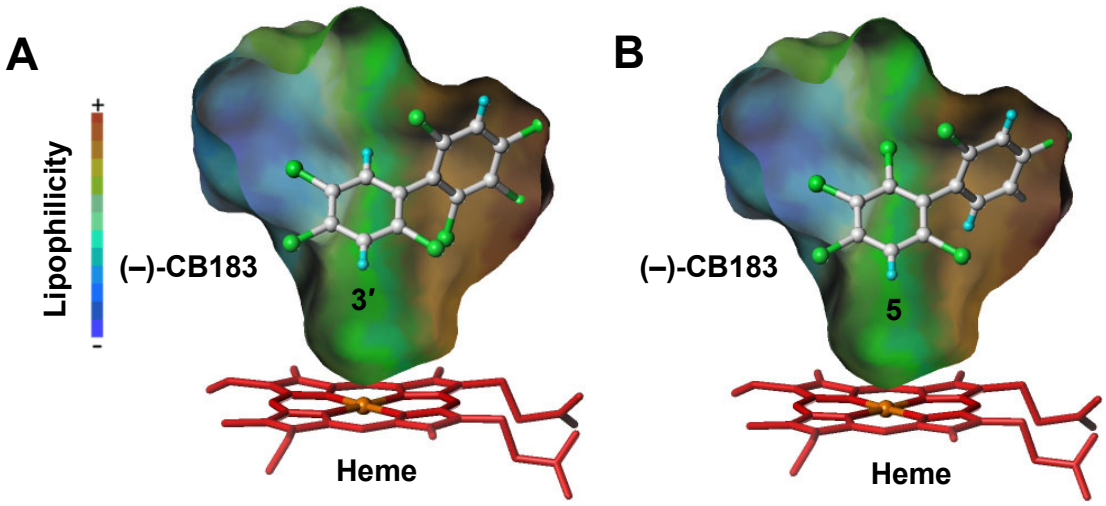

Figure 6 Preferential metabolism at 3′-position of CB183 by human CYP2B6.
(A) and (B): Docking models that 3′- and 5-positions of (–)-CB183 are facing to the heme in the binding cavity, respectively. Blue and green spheres in CB183 indicate the hydrogen and chlorine atoms, respectively. Blue and red circles on CB183 indicate the trichlorophenyl ring and tetrachlorophenyl ring, respectively.